spd tight-binding model of magnetism in transition metals: Application to Rh and Pd clusters and slabs

C. Barreteau*
Commissariat à l'Energie Atomique, DSM/DRECAM/SRSIM, Centre d'Etudes de Saclay, F-91191 Gif sur Yvette, France

R. Guirado-López and D. Spanjaard
Laboratoire de Physique des Solides, Université Paris Sud, Batiment 510, F-91405 Orsay, France

M. C. Desjonquères
Commissariat à l'Energie Atomique, DSM/DRECAM/SRSIM, Centre d'Etudes de Saclay, F-91191 Gif sur Yvette, France

Andrzej M. Oleś
Institute of Physics, Jagellonian University, Reymonta 4, PL-30059 Kraków, Poland
(Received 22 June 1999; revised manuscript received 29 September 1999)

An efficient *spd* tight-binding model is extended to the case of spin-polarized materials by including electron-electron interactions in a multiband Hubbard model treated in the Hartree-Fock approximation. The tight-binding parameters are determined from a fit to bulk *ab initio* calculations, whereas the Coulomb and exchange integrals are derived from calculations on free atoms and reduced by constant factors to take metallic screening into account. We apply our method to rhodium and palladium clusters and slabs. The results are compared with first-principle calculations and experiments. The agreement is excellent and thus this method should be very useful to study complex structures, extended defects, and large clusters. This possibility is illustrated on large Rh and Pd clusters containing up to 201 atoms.

I. INTRODUCTION

The study of magnetic properties of low-dimensional systems is nowadays one of the most important fields in solid-state physics and material sciences. This field includes the magnetism of clusters, supported or not, thin films, surfaces, multilayer systems, etc., and is of prime interest for its technological applications in magnetic recording, for instance. From a theoretical point of view, two main types of approaches have been used: (i) first-principle calculations based on the spin-polarized density-functional theory (DFT), and (ii) semiempirical methods using a tight-binding description of the bands and a Hubbard Hamiltonian accounting for the electron-electron interactions, the latter being usually treated in the Hartree-Fock approximation (HFA). The *ab initio* methods are recognized to be most often quite reliable but they are limited to very small or highly symmetrical systems. On the contrary, much larger systems can be treated using the tight-binding approach. Moreover, by introducing physically pertinent parameters, it often allows to identify which of them are responsible for the observed physical properties.

Among magnetic materials transition metals play a prominent role. In addition to the well-known ferromagnetic (FM) metals Fe, Co, and Ni, it has been shown in the last decade that some transition elements that are not magnetic in the bulk may become magnetic when the dimensionality is reduced, i.e., at surfaces or in clusters and thin films.[1,2] In particular, large magnetic moments have been observed in Rh_N clusters ($N<80$) while Pd_N clusters are not, or hardly, magnetic.[3–5] This has stimulated a lot of theoretical works based either on spin-polarized DFT (Refs. 6–15) or on the tight-binding approximation.[16–21] In the latter case the Hamiltonian is most often limited to *d* states and the number of *d* electrons is a parameter that may be crucial, in particular in clusters.[20] Thus, it is important to introduce *sp* electrons that, although weakly spin-polarized, may play a significant role in magnetism by fixing the number of *d* electrons, through the $sp-d$ hybridization. We will see in the following that this explains the discrepancy between experiments and pure *d* basis calculations, which predicted the existence of a noticeable magnetic moment in small Pd clusters.[16]

We have recently developed a tight-binding model that uses a basis set including *spd* valence atomic orbitals limited to nonmagnetic (NM) systems, and is able to reproduce quite accurately *ab initio* results for surfaces and small NM clusters.[22] The aim of the present paper is to generalize this model to magnetic materials and to demonstrate that it can handle large systems, out of reach of *ab initio* calculations at the present time, while keeping the same degree of confidence as in the latter methods. Thus, it will be shown on the specific example of Pd and Rh clusters that the results obtained using our generalized model compare favorably with those obtained from local spin density approximation (LSDA) or generalized gradient approximation (GGA) for $N\leqslant 19$, and the strength of the method for treating extended systems will be illustrated by investigating large Rh and Pd clusters up to 201 atoms. The appearance of magnetism at surfaces of elements that are not magnetic in the bulk has also been investigated both theoretically[23–30] and experimentally,[31–34] in particular for Pd(001) and Rh(001) since bulk Pd and Rh are very close to satisfying the Stoner

criterion for ferromagnetism. As a consequence we also study Rh(001), Rh(011), and Pd(001) slabs and compare our results with existing *ab initio* calculations.[29,30]

The paper is organized as follows. In Sec. II, we recall the main features of the NM *spd* tight-binding model, which is then implemented to take electron-electron interactions explicitly into account. The choice of parameters for Rh and Pd is discussed in detail in Sec. III and checked on the onset of magnetism when the lattice is expanded, by comparison to the DFT calculations. Section IV presents our results for small aggregates of Rh and Pd, and a comparison of our results with LDA and GGA calculations. Section V is devoted to the magnetism of surfaces and slabs. Finally, after a short summary, conclusions are drawn in Sec. VI.

II. THE MODEL

A. Tight-binding method in an *spd* basis set

Our tight-binding model, which can be applied to any transition metal, has been described extensively in a previous publication,[22] thus we will only briefly recall its main features. We use a minimal orthogonal basis set containing *s*, *p* and *d* real valence orbitals $|i\lambda\rangle$ centered at each site *i* ($\lambda = s,x,y,z,xy,yz,zx,x^2-y^2,3z^2-r^2$). The crystal potential is written as a superposition of spherically symmetric atomic potentials centered at each site. The Hamiltonian,

$$H_0 = T + \sum_i V(|\mathbf{r}_i - \mathbf{R}_i|) = T + \sum_i V_i , \tag{2.1}$$

has on-site and off-site matrix elements. In the off-site matrix elements three-center integrals are neglected, i.e., we include only the two-site hopping elements,

$$\beta_{i\lambda,j\mu} \equiv \langle i\lambda|H|j\mu\rangle = \langle i\lambda|V_i|j\mu\rangle. \tag{2.2}$$

Since V_i is spherically symmetric, the (9×9) matrix of hopping integrals between sites *i* and *j* is completely determined by ten Slater-Koster hopping parameters $\{ss\sigma, sp\sigma, sd\sigma, pp\sigma, pp\pi, pd\sigma, pd\pi, dd\sigma, dd\pi, dd\delta\}$ depending on the bond length R_{ij}, and by the direction cosines $\{l,m,n\}$ of the bond.[35] The Slater-Koster parameters β^{SK} are assumed to vary exponentially with distance,

$$\beta^{SK}(R_{ij}) = \beta_0^{SK} \exp\left[-q_\beta\left(\frac{R_{ij}}{R_0}-1\right)\right] f_c(R_{ij}), \tag{2.3}$$

where β_0^{SK} is the numerical value of β^{SK} at the bulk equilibrium nearest-neighbor distance R_0. The parameter q_β is taken to depend only on the angular momentum of the orbitals involved, i.e., there are six q_β parameters: q_{ss}, q_{sp}, q_{sd}, q_{pp}, q_{pd}, q_{dd}. Finally, $f_c(R)$ is a cut-off function,

$$f_c(R) = \{1 + \exp[(R-R_c)/\Delta]\}^{-1}. \tag{2.4}$$

R_c and Δ determine, respectively, the cut-off distance and the steepness of the cut off.

Let us now discuss the on-site matrix elements and consider first the case of perfectly periodic systems. Similarly to Mehl and Papaconstantopoulos[36] we assume that at each interatomic distance the reference energy is chosen in such a way that we can write the total energy E_{tot} as the sum of the occupied one electron eigenvalues ϵ_n. The on-site matrix elements of *H* are assumed to depend only on the angular momentum of the considered orbitals and are given by ($\lambda = s,p,d$),[36]

$$\varepsilon_{i\lambda}^0 = a_\lambda + b_\lambda \rho_i^{2/3} + c_\lambda \rho_i^{4/3} + d_\lambda \rho_i^2 . \tag{2.5}$$

The function ρ_i depends on the local environment and is defined as

$$\rho_i = \sum_{j\neq i} \exp\left[-p_\rho\left(\frac{R_{ij}}{R_0}-1\right)\right] f_c(R_{ij}). \tag{2.6}$$

This introduces thirteen new parameters.

Thus, to completely specify our model we need to determine twenty nine parameters. This is carried out using a nonlinear least mean square fitting of bulk band structure and total energy *ab initio* [augmented spherical wave (ASW) code[37]] calculations for a set of interatomic distances and two atomic structures with different coordinations (fcc, bcc).

When dealing with systems in which all atoms are not equivalent an additional shift δV_i must be added to the on-site terms $\varepsilon_{i\lambda}^0$. This shift is determined self-consistently to insure a local charge neutrality.[22] The total energy must then be modified so that electron-electron interactions are not counted twice, the total energy then reads,

$$E_{tot} = \sum_{n\,occ} \epsilon_n - N_{val} \sum_i \delta V_i , \tag{2.7}$$

where N_{val} is the total number of *spd* valence electrons per atom of the transition metal.

B. Electron-electron interaction

In the previous section, we presented a method based on a realistic Hamiltonian to study the electronic properties of NM transition metals. In this section, this method is extended in order to take into account magnetic effects in the framework of a multiband Hubbard model, treated in the Hartree-Fock approximation. For this purpose, we use the second quantization formalism ($c_{i\lambda\sigma}^\dagger$ and $c_{i\lambda\sigma}$ are the creation and annihilation operators of an electron in the spin orbital $|i\lambda\sigma\rangle$ of spin σ, $n_{i\lambda\sigma}$ is the occupation number operator of the spin orbital $|i\lambda\sigma\rangle$) and rewrite our NM Hamiltonian H_0 (2.1) as follows,

$$H_0 = \sum_{i\lambda\sigma} \varepsilon_{i\lambda}^0 n_{i\lambda\sigma} + \sum_{\substack{i\lambda,j\mu,\sigma \\ i\neq j}} \beta_{i\lambda,j\mu} c_{i\lambda\sigma}^\dagger c_{j\mu\sigma} - N_{val} \sum_i \delta V_i . \tag{2.8}$$

It is well known that the charge redistribution of the spin-polarized system is determined mainly by intra-atomic Coulomb ($U_{\lambda\mu}$) and exchange ($J_{\lambda\mu}, \lambda\neq\mu$) interactions:

$$U_{\lambda\mu} = \langle \phi_{i\lambda}(\mathbf{r})\phi_{i\mu}(\mathbf{r}')| \frac{1}{|\mathbf{r}-\mathbf{r}'|} |\phi_{i\lambda}(\mathbf{r})\phi_{i\mu}(\mathbf{r}')\rangle, \tag{2.9}$$

$$J_{\lambda\mu}=\langle\phi_{i\lambda}(\boldsymbol{r})\phi_{i\mu}(\boldsymbol{r}')|\frac{1}{|\boldsymbol{r}-\boldsymbol{r}'|}|\phi_{i\mu}(\boldsymbol{r})\phi_{i\lambda}(\boldsymbol{r}')\rangle$$

$$=\langle\phi_{i\lambda}(\boldsymbol{r})\phi_{i\lambda}(\boldsymbol{r}')|\frac{1}{|\boldsymbol{r}-\boldsymbol{r}'|}|\phi_{i\mu}(\boldsymbol{r}')\phi_{i\mu}(\boldsymbol{r})\rangle. \tag{2.10}$$

All integrals involving more than two orbitals (three or four) are neglected. Let us also recall the important relation between Coulomb and exchange integrals, which holds for any pair of λ and μ referring to the same type of orbitals (p or d):

$$U_{\lambda\lambda}=U_{\lambda\mu}+2J_{\lambda\mu},\quad \forall\lambda\neq\mu. \tag{2.11}$$

In order to reduce the number of parameters we will consider only the average values of $U_{\lambda\mu}$ and $J_{\lambda\mu}$ ($\lambda\neq\mu$), such that we have six Coulomb integrals: U_{ss}, U_{sp}, U_{sd}, $U_{pp'}$, U_{pd}, $U_{dd'}$, and five exchange integrals: J_{sp}, J_{sd}, $J_{pp'}$, J_{pd}, $J_{dd'}$, with $p'\neq p$ and $d'\neq d$. The intra-atomic electron-electron interaction in second quantization can be written in the form,

$$H_{int}=\tfrac{1}{2}\sum_{i\lambda\sigma}U_{\lambda\lambda}n_{i\lambda,-\sigma}n_{i\lambda\sigma}+\tfrac{1}{2}\sum_{\substack{i\lambda\mu,\lambda\neq\mu\\ \sigma\sigma'}}U_{\lambda\mu}n_{i\mu\sigma'}n_{i\lambda\sigma}$$

$$+\tfrac{1}{2}\sum_{\substack{i\lambda\mu,\lambda\neq\mu\\ \sigma\sigma'}}J_{\lambda\mu}c^{\dagger}_{i\lambda\sigma}c^{\dagger}_{i\mu\sigma'}c_{i\lambda\sigma'}c_{i\mu\sigma}$$

$$+\tfrac{1}{2}\sum_{\substack{i\lambda\mu,\lambda\neq\mu\\ \sigma}}J_{\lambda\mu}c^{\dagger}_{i\lambda\sigma}c^{\dagger}_{i\lambda,-\sigma}c_{i\mu,-\sigma}c_{i\mu\sigma}. \tag{2.12}$$

C. Hartree-Fock approximation

In the standard HFA H_{int} becomes,

$$H^{\mathrm{HF}}_{int}=\sum_{i\lambda\sigma}\Bigg[U_{\lambda\lambda}\langle n_{i\lambda,-\sigma}\rangle+\sum_{\substack{\mu\neq\lambda\\ \sigma'}}U_{\lambda\mu}\langle n_{i\mu\sigma'}\rangle$$

$$-\sum_{\mu\neq\lambda}J_{\lambda\mu}\langle n_{i\mu\sigma}\rangle\Bigg]n_{i\lambda\sigma}-\sum_{\substack{i\lambda\mu,\lambda\neq\mu\\ \sigma}}[(U_{\lambda\mu}-J_{\lambda\mu})$$

$$\times\langle c^{\dagger}_{i\lambda\sigma}c_{i\mu\sigma}\rangle-2J_{\lambda\mu}\langle c^{\dagger}_{i\lambda,-\sigma}c_{i\mu,-\sigma}\rangle]c^{\dagger}_{i\mu\sigma}c_{i\lambda\sigma}, \tag{2.13}$$

where $\langle n_{i\lambda\sigma}\rangle$ is the average occupation of the spin orbital $|i\lambda\sigma\rangle$. Therefore, H^{HF}_{int} can be written as a purely local ''one-electron'' Hamiltonian,

$$H^{\mathrm{HF}}_{int}=\sum_{i\lambda\sigma}\Delta\varepsilon_{i\lambda\sigma}n_{i\lambda\sigma}+\sum_{\substack{i\lambda\mu,\lambda\neq\mu\\ \sigma}}h_{i\lambda,i\mu,\sigma}c^{\dagger}_{i\mu\sigma}c_{i\lambda\sigma}. \tag{2.14}$$

$\Delta\varepsilon_{i\lambda\sigma}$ are the renormalization of on-site levels depending on the local atomic environment via the average occupations of the spin orbitals $\langle n_{i\lambda\sigma}\rangle$ due to Coulomb ($U_{\lambda\mu}$) and exchange ($J_{\lambda\mu}$) interactions. The Fock terms $h_{i\lambda,i\mu,\sigma}$ are on site but interorbital hopping integrals, which vanish in the bulk but should be taken into account when the symmetry is reduced.[16]

Finally, double counting terms $E_{dc}=\langle H^{HF}_{int}\rangle/2$ must be subtracted from the sum of occupied one electron energies in order not to count twice electron-electron interactions in the total energy.

At this point, it is important to note that for any geometrical configuration the HF renormalization of the energy levels and the Fock terms are implicitly included in the on-site parameters of a NM state. However, other effects are also involved in the variation of these parameters so that it is convenient to take the NM state as a reference. The Hamiltonian in a magnetic situation can then be written as a perturbation with respect to the NM case for the same geometrical configuration, such that we have,

$$H=H_0+H'^{\mathrm{HF}}_{int}-E'_{dc}, \tag{2.15}$$

where the terms H'^{HF}_{int} and E'_{dc} contain the contribution to the total energy due to the charge redistribution induced by a magnetic symmetry breaking. H'^{HF}_{int} can then be written as follows,

$$H'^{\mathrm{HF}}_{int}=H^{\mathrm{HF}}_{int}-H^{0,\mathrm{HF}}_{int}, \tag{2.16}$$

H^{HF}_{int} and $H^{0,\mathrm{HF}}_{int}$ are given by Eq. (2.13) in which the average operators refer to the magnetic and NM configurations, respectively. The same type of relation (with the same notations) can be written for the double counting term as follows,

$$E'_{dc}=E_{dc}-E^{0}_{dc}. \tag{2.17}$$

Before concluding this section, we would like to make a few comments on the calculation method: (i) The average intraorbital ($\langle n_{i\lambda\sigma}\rangle$) and interorbital ($\langle c^{\dagger}_{i\lambda\sigma}c_{i\mu\sigma}\rangle$) occupations must be determined self'consistently. In all our magnetic calculations input and output average occupations are mixed with a weight as large as 0.3–0.5 on input data and the iterations are stopped whenever the difference between two successive average intraorbital occupations is less than 10^{-6}. This choice is found to be the most appropriate. (ii) In magnetic systems many stable or metastable solutions often exist. A good way of ''exploring'' the different magnetic configurations is to start from the NM density configuration and to break the symmetry by adding a magnetic field at the first iteration (which is reduced to zero along the iteration process). Depending on the strength of the initial magnetic field, such a procedure may lead to different magnetic configurations. (iii) The potential correction δV_i, which insures local charge neutrality is determined in the NM system, but no local neutrality condition is imposed in the magnetic system. In the latter case, the charge redistribution is determined self-consistently keeping the same value of δV_i, and therefore some charge transfer may occur. In practice, these charge transfers remain small and the system is almost locally neutral, except in some very peculiar cases. (iv) In the present semiempirical method the interaction parameters $U_{\lambda\mu}$ and $J_{\lambda\mu}$ have to be understood as effective *screened* parameters. In this respect, they have a similar meaning to

TABLE I. The parameters (in eV) determining the on-site *s*, *p*, *d* matrix elements of the tight-binding Hamiltonian for rhodium and palladium in the absence of spin polarization. The value of p_ρ in Eq. (2.6) is $p_\rho=9.527$ for rhodium and $p_\rho=8.800$ for palladium. The reference energy of these matrix elements has been chosen such that the total energy per bulk atom at equilibrium in the fcc structure is the opposite of the experimental cohesive energy (5.78 eV for rhodium, 3.91 eV for palladium).

Atom	Orbital	a_α	b_α	c_α	d_α
Rh	*s*	1.3329	3.0637	−0.1788	0.0069
	p	6.1674	2.9454	−0.2247	0.0094
	d	0.1259	−0.0370	0.0233	−0.0009
Pd	*s*	1.4776	2.6065	−0.2288	0.011
	p	5.9799	2.8100	−0.2071	0.0009
	d	0.0774	−0.0774	0.0211	−0.0008

those used in the so-called LDA+*U* method.[38] The reason to treat these parameters as effective ones is due to the neglect of correlation effects.

III. DETERMINATION OF PARAMETERS

In the present section, we explain the procedure used for the determination of the parameters. First, the purely tight-binding parameters, on-site orbital energies $\varepsilon^0_{i\lambda}$ and hopping integrals $\beta_{i\lambda,j\mu}$ and, secondly, the Coulomb and exchange integrals, $U_{\lambda\mu}$ and $J_{\lambda\mu}$.

A. Tight-binding parameters

The parameters for rhodium and palladium[22,39] are recalled in Tables I and II. For both elements the steepness of the cut off Δ is chosen equal to 0.15 Å , and the cut off R_c is 5.5 Å for rhodium and 5.6 Å for palladium, since the equilibrium nearest-neighbor distance of palladium is about 2% larger than that of rhodium. As shown in our previous papers they give an accurate description of the electronic structure and total energy for various systems such as bulk, surfaces, and clusters proving their adequacy and their high transferability.

B. Atomic Coulomb and exchange integrals

The various Coulomb and exchange integrals have been determined from their atomic values and then reduced by screening factors. In order to obtain these atomic parameters a self-consistent LDA calculation has been performed for the free atoms in several chosen atomic configurations giving the corresponding atomic levels. Following the HFA point of view developed in Sec. II C, these atomic levels can be written as linear combinations of the *total* occupation numbers: $n_{s\sigma}$, $n_{p\sigma}$, and $n_{d\sigma}$ of the valence atomic spin orbitals of character *s*, *p*, and *d*, respectively, the coefficients of which are actually the interaction parameters to be determined. However, since in the LDA formalism the self interactions are not suppressed, we write these linear combinations including the self-interaction terms as follows,

$$\varepsilon_{s\sigma}=\varepsilon^0_s+U_{ss}n_s+U_{sp}n_p+U_{sd}n_d-J_{sp}n_{p\sigma}-J_{sd}n_{d\sigma}, \tag{3.1}$$

$$\varepsilon_{p\sigma}=\varepsilon^0_p+U_{sp}n_s+U_{pp'}n_p+U_{pd}n_d-J_{sp}n_{s\sigma}-\tfrac{1}{3}J_{pp'}n_{p\sigma}+\tfrac{2}{3}J_{pp'}n_{p,-\sigma}-J_{pd}n_{d\sigma}, \tag{3.2}$$

$$\varepsilon_{d\sigma}=\varepsilon^0_d+U_{sd}n_s+U_{pd}n_p+U_{dd'}n_d-J_{sd}n_{s\sigma}-J_{pd}n_{p\sigma}-\tfrac{3}{5}J_{dd'}n_{d\sigma}+\tfrac{2}{5}J_{dd'}n_{d,-\sigma}, \tag{3.3}$$

with $n_\lambda=n_{\lambda\sigma}+n_{\lambda,-\sigma}$ and $\lambda=s,p,d$.

In order to reduce the number of independent parameters we have only considered *sd* configurations and fixed the ratio $U_{ss}/U_{dd'}=0.32$. The parameters U_{sd}, $U_{dd'}$, J_{sd}, and $J_{dd'}$ have then been derived from a linear least mean square

TABLE II. The Slater-Koster hopping integrals (in eV) at the bulk fcc equilibrium nearest-neighbor distance R_0 and the corresponding parameters q_β governing their variation with distance [see Eq. (3)].

	Rhodium		Palladium	
	β^{SK}_0	q_β	β^{SK}_0	q_β
$ss\sigma$	−0.9755	2.2556	−0.7396	1.9994
$sp\sigma$	1.9945	2.9709	1.7622	2.7889
$sd\sigma$	−0.9488	2.6455	−0.7224	2.6146
$pp\sigma$	3.3313	3.1266	3.2648	3.3568
$pp\pi$	−0.1218	3.1266	−0.0822	3.3568
$pd\sigma$	−1.3096	3.7810	−1.0253	3.8409
$pd\pi$	0.1561	3.7810	0.1462	3.8409
$dd\sigma$	−0.9132	4.8526	−0.7078	4.9264
$dd\pi$	0.5176	4.8526	0.4175	4.9264
$dd\delta$	−0.0806	4.8526	−0.0736	4.9264

TABLE III. Coulomb $U_{\lambda\mu}$ and exchange $J_{\lambda\mu}$ integrals (in eV) obtained from an atomic calculation and screened, respectively, by a factor $\alpha_U=0.2$ and $\alpha_J=0.7$ ($U_{pp}=U_{pp'}+2J_{pp'}$, $U_{dd}=U_{dd'}+2J_{dd'}$).

$U_{\lambda\mu}$	Rh	Pd	$J_{\lambda\mu}$	Rh	Pd
U_{ss}	0.340	0.384			
U_{sp}	0.204	0.231	J_{sp}	0.143	0.161
U_{sd}	0.516	0.575	J_{sd}	0.114	0.110
$U_{pp'}$	0.204	0.230	$J_{pp'}$	0.178	0.202
U_{pd}	0.413	0.460	J_{pd}	0.091	0.088
$U_{dd'}$	1.061	1.201	$J_{dd'}$	0.399	0.415

fit of the LDA atomic levels. The Coulomb and exchange integrals involving *p* orbitals have been assumed to obey the following relations: $U_{sp}=3U_{ss}/5$, $U_{pp'}=U_{sp}$, $U_{pd}=2U_{pp'}$, $J_{sp}=U_{sp}/5$, $J_{pp'}=U_{sp}/4$, $J_{pd}=4J_{sd}/5$. Note that the most important parameters are $U_{dd'}$ and $J_{dd'}$; we have checked that those involving *s* and *p* orbitals are not crucial provided that they have the correct order of magnitude since the occupation numbers n_s and n_p are small (i.e., only a fraction of an electron) in transition metals.

C. Determination of screening factors

In the previous section, we described the procedure to determine the atomic Coulomb and exchange interactions of the atom. In an extended system it is necessary to screen these intra-atomic interactions[40] in a standard HFA to simulate the realistic situation in transition metals (in particular the missing correlation effects). Since it is known that Coulomb interactions are much more screened than exchange interactions,[41] we will introduce two screening multiplicative factors, α_U and α_J, operating respectively on the *U* and *J* atomic values. These parameters are expected to lie within the range of 0.2–0.3 for α_U and 0.6–1.0 for α_J. In order to estimate α_U and α_J we have chosen a physical system that is known to present a drastic magnetic change at a precise value of the interatomic spacing, and then adjusted the screening to reproduce this magnetic transition.

1. Palladium

It is known that palladium has a very large bulk magnetic susceptibility, and even though palladium is NM at the equilibrium lattice constant, an abrupt NM/FM phase transition occurs for a rather small lattice expansion. Using the ASW code with the spin-polarized von Barth-Hedin exchange and correlation function,[42] palladium (fcc) is found to be NM at the equilibrium distance, but for an expansion of only 3% (lattice parameter of 4.0 Å) a small magnetic moment appears, which increases abruptly up to a value of $0.36\mu_B$ per atom for an 11% expansion (lattice parameter of $\sim$4.3 Å), after which it saturates.

By performing tight-binding calculations around the equilibrium lattice constant for several screening parameters α_U and α_J we have found that $\alpha_U=0.20$ and $\alpha_J=0.70$ is a good choice (the corresponding values of the Coulomb and exchange integrals are given in Table III). Indeed, with these values, we reproduce closely the variation of the magnetic moment as a function of the Wigner-Seitz radius that we have obtained from the *ab initio* ASW code, using the same 60 special **k** points in the irreducible part of the Brillouin zone (IBZ); for instance, saturation of the moment occurs for the same lattice expansion in both calculations (Fig. 1).

Moreover in the HFA for a pure *d* band in which all orbitals are assumed to be equivalent, the Stoner parameter is given by $I=(U_{dd'}+6J_{dd'})/5$ (Ref. 43), which, with the chosen values of α_U and α_J, is equal to 0.738 eV. This value is rather close to $I=0.67$ eV, which can be derived from the density of states per atom and per spin at the Fermi level, $n(E_F)$, and from the susceptibility enhancement, $\chi/\chi_0=(1-In(E_F))^{-1}$, given by Moruzzi, Janak, and Williams.[44]

Finally these magnetic transitions under expansion have been investigated by Moruzzi *et al.*[45,46] on several transition metals using an ASW code and the von Barth-Hedin functional as we did. Calculations were performed for palladium and rhodium,[46] up to a very large volume (more than 100% expansion). Another check of our estimation of screening factors is to verify that our model reproduces correctly these calculations.

In Fig. 1, we show our results for palladium. The magnetization curve is extremely similar to the one obtained by Moruzzi and Marcus in Fig. 2 of their paper:[46] the transition from a NM to a FM state occurs abruptly for expansions of 3–6 % and then the magnetic moment *decreases* more slowly towards zero, which corresponds to the atomic NM $4d^{10}$ configuration. Note however that the total magnetic moment is slightly smaller in our model, and the FM solution disappears for a somewhat shorter distance. This can be due to technical details of the calculation. In particular, these authors give no information on the number of **k**-points they

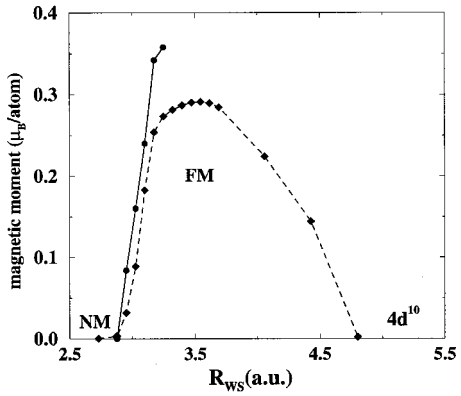

FIG. 1. The nonmagnetic (NM)-ferromagnetic(FM) transition in Pd under lattice expansion (R_{ws} is the Wigner-Seitz radius, $R_{ws}=2.87$ a.u. at equilibrium). Full line (with circles): *ab initio* ASW results; dashed line (with squares): tight-binding Hartree-Fock results. The screening factors are $\alpha_U=0.2$ and $\alpha_J=0.7$.

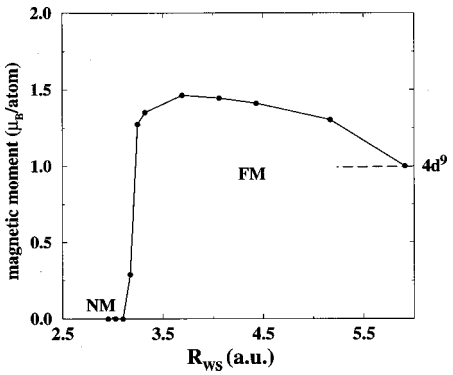

FIG. 2. The nonmagnetic (NM)-ferromagnetic(FM) transition in Rh under lattice expansion (R_{ws} is the Wigner-Seitz radius, $R_{ws}=2.81$ a.u. at equilibrium) obtained from the tight-binding Hartree-Fock model. The screening factors are $\alpha_U=0.2$ and $\alpha_J=0.7$.

used. This could change significantly the value of the magnetic moment as will be pointed out in the following (see Sec. V). Nevertheless, the overall agreement can be considered as very satisfactory.

2. Rhodium

Rhodium is very interesting to compare to palladium since it is located just before this metal in the periodic table. The shapes of their bulk densities of states are extremely similar since they have the same (fcc) bulk structure. However, the Fermi energy of rhodium lies well below a sharp peak, while the Fermi energy of palladium lies just above this peak. It is therefore expected that magnetism should appear for a larger expansion in rhodium than in palladium. In addition, contrary to palladium, which is NM as a free atom, atomic rhodium has the configuration $4d^8 5s^1$ and its magnetic moment should approach $3\mu_B$ at very large interatomic spacings.

We performed calculations for rhodium similar to the ones of palladium, with the Coulomb and exchange integrals given in Table III obtained from the atomic values with the same screening coefficients as for palladium [note that with these values $I=0.69$ eV to be compared to 0.65 eV obtained from $n(E_F)$ and χ/χ_0 given in Ref. 44]. The result of our calculation is shown in Fig. 2 to be compared with Fig. 1 of Moruzzi and Marcus,[46] the similarity of the two curves is striking; there is a steep transition from a NM to a FM state for an expansion around 13–16 %, the magnetic moment reaches a maximum and then decreases slowly towards the ''atomic'' value of $1\mu_B$ in both calculations. This last value corresponds to an atomic configuration $4d^9$, which is also found in most DFT calculations,[13,15,44,46] and not to the experimental one $4d^8 5s^1$. However, computations reveal that the energies of these two configurations are very close.[13,15]

3. Discussion

By assuming that the values of the Coulomb and exchange integrals do not change with distance (same screening for all distances), we have been able to reproduce very closely the results of *ab initio* calculations on the variations of the magnetic moment within a very broad range of interatomic distances for Rh and Pd. This approximation, which is most often used, is based on the local nature of screening. This argument also suggests that the same screening factors are also valid for various geometrical environments, i.e., in systems as different from the bulk as clusters and slabs. Note also that the same screening factors lead to equally good results for both metals.

IV. APPLICATION TO SMALL AGGREGATES OF RHODIUM AND PALLADIUM

We have applied our model to the study of small Rh_N and Pd_N clusters with $2<N<201$. We will consider first clusters in which all atoms are geometrically equivalent, i.e., the charge transfer is absent and thus $\delta V_i=0$. Then, we will extend our study to clusters with inequivalent atoms.

A. Aggregates with geometrically equivalent atoms

The clusters we have investigated are ($X=$Rh or Pd): the dimer X_2, the equilateral triangle X_3, the square X_4^{sq} and the regular tetrahedron X_4^{tet}, the regular octahedron X_6^{octa} and, finally, the hollow icosahedron X_{12}^{ico} and cubooctahedron X_{12}^{cubo} (i.e., without a central atom). For each cluster the total energy has been minimized with respect to the nearest-neighbor distance, and all the possible self-consistent magnetic solutions have been systematically searched. Let us note that sometimes a self-consistent magnetic solution is found but becomes unstable before reaching the equilibrium bond length. The set of results concerning the binding energy E (eV/atom), the contraction of nearest neighbor distances $\Delta R/R_o$ and the magnetic moment M (in μ_B/atom), is given in Tables IV and V for Rh and Pd, respectively. It is observed that Rh_N clusters are most often magnetic in the ground state and, in many cases, other (metastable) magnetic solutions exist which may be quite close in energy (Fig. 3). On the contrary, Pd_N clusters are NM or carry only small magnetic moments and no metastable magnetic solution is found.

For all clusters and self-consistent solutions a contraction of the equilibrium bond length with respect to the bulk one is obtained. This contraction decreases: (i) in the ground state when N increases since the average coordination increases,[47] (ii) for a given cluster when the magnetic moment increases (Fig. 3) since for these elements belonging to the second half of the $4d$ series magnetism tends to fill more antibonding majority spin states at the expense of less antibonding minority spin ones. It follows from these considerations that the search of the equilibrium bond length should be done simultaneously with the determination of the magnetic state, which is not always the case in *ab initio* calculations. The binding energy per atom increases with the average coordination. As a consequence, when two isomers are compared, the most stable one has the structure with the highest coordination (tetrahedron for Rh_4 and Pd_4, icosahedron for Rh_{12} and Pd_{12}) and, thus, the lowest bond length contraction.

As expected, our results show that spin polarizations are always largely dominated by d electrons, the s and p contributions being quite small, most often less than $0.01\mu_B$ with an opposite sign (Tables VI and VII). For Pd_N the $4d$ shell tends to become completely filled (since the free atom configuration is $4d^{10}$) when the size decreases. This plays against magnetism at very small sizes and, since bulk Pd is

TABLE IV. The binding energy per atom E (in eV), the bond length contraction $\Delta R/R_0$ (in %) of the equilibrium nearest-neighbor distance R in the cluster relative to the bulk one and the average magnetic moment M (μ_B/atom) for Rh_N clusters in the ground state and all metastable solutions. $\langle Z \rangle$ is the average coordination. In the case (denoted by an asterisk) where all first nearest-neighbor distances are not identical, we have counted as first neighbors all atoms located at less than $1.1R$ of a given atom. In Rh_9 and Rh_{19}^{ico} there are several interatomic distances in a range of 15% and it is hard to define an average coordination. In Rh_{19}^{ico}, R is the distance between a central atom and one of its neighbors on the surface.

Cluster	$\langle Z \rangle$	E	$\Delta R/R_0$	M
clusters with equivalent atoms				
Rh_2	1.0	1.488	16.5	1.000
		1.477	17.6	0.000
Rh_3	2.0	2.034	10.9	0.333
		1.955	9.8	1.000
Rh_4^{sq}	2.0	2.180	11.4	0.000
		2.118	11.0	0.500
Rh_4^{tetra}	3.0	2.370	7.5	0.000
		2.369	7.3	0.500
		2.293	5.6	1.500
Rh_6^{octa}	4.0	3.251	5.0	1.333
		3.244	5.4	1.000
		3.129	5.9	0.000
Rh_{12}^{ico}	5.0	3.398	3.3	1.166
		3.391	3.8	0.666
		3.330	4.0	0.000
Rh_{12}^{cubo}	4.0	3.124	5.5	1.000
		2.990	5.7	0.000
clusters with inequivalent atoms				
Rh_7^{dipyr}	4.57*	3.246	3.8	1.285
		3.190	4.6	0.143
Rh_8^{mtw}	4.50	3.047	3.4	1.250
		2.991	4.2	0.250
		2.971	4.2	0.000
Rh_9^{bcc}		2.914	8.8	0.555
Rh_{10}^{twp}	4.80	3.442	4.0	1.000
		3.438	3.8	1.200
		3.409	4.5	0.000
		3.408	4.5	0.200
Rh_{13}^{ico}	6.46*	3.847	4.8	1.153
		3.799	5.1	0.692
		3.748	5.2	0.076
Rh_{13}^{cubo}	5.54	3.631	2.9	1.000
Rh_{19}^{ico}		3.984	3.6	1.105
		3.973	3.9	0.684

not magnetic, explains why Pd clusters have only a weak tendency to magnetism. In Rh_N clusters, the number of electrons in the $4d$ states also increases as N decreases, and the electronic configuration approaches $4d^9$, which, as already stated, is the most often found configuration in density-functional calculations.[13,15,44,46] As a result, we find that the atoms of the dimer carry a magnetic moment of $1\mu_B$ per atom instead of the experimental value $2\mu_B$.[5] Nevertheless, we will see in the following that for other clusters our results are very close to LDA and GGA calculations.

B. Aggregates with geometrically unequivalent atoms

Let us now consider clusters where all atoms are not geometrically equivalent. We have chosen to focus our attention on several highly coordinated clusters such as the pentagonal dipyramid X_7^{dipyr}, the multitwin tetrahedral X_8^{mtw} (built from a regular tetrahedron to which an atom is added on each facet at a threefold position), the centered cube X_9^{bcc}, the twisted double square pyramid X_{10}^{twp} (built from two squares twisted by 45° and with an atom added on each square face), the

TABLE V. Same caption as Table IV but for Pd_N clusters.

Cluster	$\langle Z \rangle$	E	$\Delta R/R_0$	M
		clusters with equivalent atoms		
Pd_2	1.0	1.145	18.9	0.000
Pd_3	2.0	1.456	12.1	0.000
Pd_4^{sq}	2.0	1.463	12.0	0.000
Pd_4^{tetra}	3.0	1.857	10.0	0.500
		1.781	10.0	0.000
Pd_6^{octa}	4.0	2.465	7.8	0.333
		2.451	7.9	0.000
Pd_{12}^{ico}	5.0	2.511	5.3	0.167
		2.502	5.3	0.000
Pd_{12}^{cubo}	4.0	2.324	7.55	0.000
		clusters with inequivalent atoms		
Pd_7^{dipyr}	4.57*	2.490	6.4	0.286
		2.457	6.4	0.000
Pd_8^{mtw}	4.50	2.314	6.0	0.250
		2.294	6.0	0.000
Pd_9^{bcc}		2.107	10.0	0.222
		2.086	10.0	0.000
Pd_{10}^{twp}	4.80	2.543	5.8	0.200
		2.529	5.8	0.000
Pd_{13}^{ico}	6.46*	2.834	6.1	0.154
		2.824	6.1	0.000
Pd_{13}^{cubo}	5.54	2.683	4.6	0.154
		2.679	4.6	0.000

icosahedron X_{13}^{ico}, the cubooctahedron X_{13}^{cubo} and the double icosahedron X_{19}^{ico}. Finally, we will consider also two larger icosahedral and cubooctahedral clusters, $X_{55}^{ico}, X_{55}^{cubo}$ and $X_{147}^{ico}, X_{147}^{cubo}$, which, to our knowledge, have not been yet studied with spin-polarized *ab initio* methods.

In Tables IV and V the binding energy E (eV/atom), the contraction of nearest-neighbor distances ($\Delta R/R_o$) and the magnetic moment M (μ_B/atom) for Rh_N and Pd_N clusters are presented. Once again several metastable solutions are found in the case of Rh_N clusters, but only solutions with a very small magnetic moment exist for Pd_N clusters, which confirms the tendency of palladium to be NM. We also note that

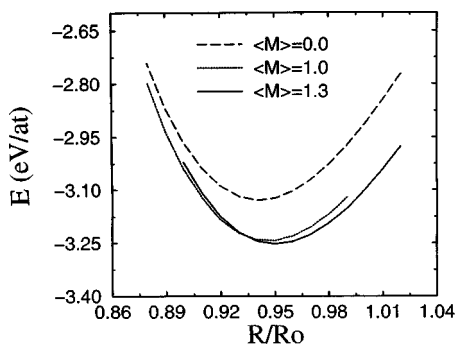

FIG. 3. Total energy (in eV/atom) as a function of R/R_o for Rh_6 clusters. R and R_o stand for the equilibrium nearest-neighbor distance in the cluster and in the bulk, respectively. All (magnetic and nonmagnetic) solutions are shown.

the total energy and interatomic distance increase almost monotonically with the average coordination and, similarly to the case of clusters with equivalent sites, the equilibrium distance is always larger for solutions with a high magnetic moment. On the contrary, the variation of magnetic moment with the size of the cluster presents sharp oscillations (see Tables IV and V), as observed experimentally.[3,4]

It is worthwhile to compare in detail the two isomers with thirteen atoms. For both elements the icosahedron is more stable than the cubooctahedron and the equilibrium nearest-neighbor distance of this last structure is in between the two nearest-neighbor distances of the icosahedron, i.e., the distance between the central atom and those of the outside shell, and the nearest-neighbor intrashell distance, which is $\simeq 5\%$ larger than the former.

Let us now discuss the magnetic properties and begin with the case of Rh_{13}. In the bulk metal for which the spectrum of electronic levels is continuous a good criterion for the appearance of magnetism is $n(E_F) > I^{-1}$ where $n(E_F)$ is the density of states at the Fermi level in the unpolarized system and I the Stoner parameter. When the spectrum is discrete, this criterion cannot be applied directly. However, it can be inferred that magnetism will be favored when, in the absence of spin polarization, the highest occupied molecular orbital (HOMO) is partly filled and its level located in a region of the electronic spectrum in which the levels are close together. This condition is fulfilled for Rh_{13} in both geometries and this explains the strong tendency to magnetism in these clusters. Unexpectedly, in both structures the

TABLE VI. The local charges and the local moments (in μ_B) of d character for Rh_N clusters in the ground state. In the case of clusters with unequivalent atoms we have labeled the types of sites by a,b (where a refers to the most coordinated atom except for Rh_{19}^{ico}), and given the corresponding local total charge $N(i)$ and magnetic moment $M(i)$ (μ_B/atom). The double icosahedron Rh_{19}^{ico} has four different sites: a refers to the two central atoms, b to the two apices, c to the five atoms first nearest neighbors of each apex, and d to the five atoms of the central pentagon.

Cluster	atom	Charge		Spin	
		n_{4d}	$N(i)$	m_{4d}	$M(i)$
		clusters with equivalent atoms			
Rh_2^{dim}		8.848		1.001	1.000
Rh_3^{tri}		8.775		0.339	0.333
Rh_4^{tetra}		8.401		0.000	0.000
Rh_4^{sq}		8.760		0.000	0.000
Rh_6^{octa}		8.489		1.340	1.333
Rh_{12}^{ico}		8.527		1.181	1.166
Rh_{12}^{cubo}		8.555		1.007	1.000
		clusters with inequivalent atoms			
Rh_7^{dipyr}	*a*	8.255	8.833	1.464	1.463
	b	8.608	9.066	1.227	1.215
Rh_8^{mtw}	*a*	8.502	9.050	1.185	1.205
	b	8.603	8.949	1.285	1.293
Rh_9^{bcc}	*a*	8.132	8.999	−0.048	−0.071
	b	8.559	9.000	0.644	0.634
Rh_{10}^{twp}	*a*	8.490	8.984	0.964	0.956
	b	8.650	9.063	1.188	1.178
Rh_{13}^{ico}	*a*	8.543	9.569	1.104	1.068
	b	8.463	8.952	1.172	1.161
Rh_{13}^{cubo}	*a*	8.377	9.322	1.252	1.211
	b	8.501	8.973	0.993	0.983
Rh_{19}^{ico}	*a(2)*	8.170	9.137	0.899	0.868
	b(2)	8.425	8.940	0.930	0.920
	c(10)	8.442	8.948	1.212	1.205
	d(5)	8.468	9.074	1.089	1.073

magnetic moment is roughly equally shared between all atoms even though the central atom is much more coordinated than those of the outside shell. Actually, the central atom, being a center of symmetry of the aggregate, has a very peculiar local electronic spectrum since the antisymmetric wave functions have no weight on it, whereas the weight of the symmetric ones is enhanced. As a result the spectrum weighted on the central atom is made of small packets of levels separated by gaps. If the HOMO falls in the middle of one packet, which is the case in Rh_{13} clusters, the central atom is likely to be magnetic.

The same comments also apply to Pd_{13}, but in these clusters the outside shell atoms have very few d holes and accordingly their local magnetic moments are very small. This result is in contrast with those of a former study[16] in which the basis set was limited to d orbitals, the number of d holes being fixed to the bulk value. Under these conditions a saturated moment ($8\mu_B$) was found. This illustrates the importance of taking sp electrons into account since they reduce the number of d holes when the cluster size decreases.

The analysis of the charge distribution on the different sites of the clusters shows that, even though the self-consistent potentials δV_i ensure the local neutrality in the NM case, the different sites of the clusters in the magnetic configuration do not remain strictly neutral. In most cases, however, the charge transfer is rather small (i.e., less than $0.15e^-$), save for the $N=13$ clusters. In this case the central atom is highly coordinated (same coordination as in the bulk), whereas the twelve peripheric atoms have a much smaller coordination. As a result, though the central atom shows a noticeable charge, this charge is taken from (or distributed over) the twelve atoms of the periphery, which remain almost neutral.

Since our Hartree-Fock tight-binding model is much less costly in computer time than standard *ab initio* methods it is easy to study extended systems. In particular it is of interest to determine when magnetism disappears as the size of cubooctahedrons and icosahedrons increases. We find that solutions with rather large magnetic moments (more than 0.3 μ_B/atom) remain stable for Rh_{55}^{ico} and Rh_{55}^{cubo} (see Table VIII), but for Rh_{147}^{cubo} the only magnetic solution has an extremely small magnetic moment of 0.037 μ_B/atom. For Rh_{147}^{ico} there are two magnetic solutions with respective magnetic moments $0.21\mu_B$ and $0.009\mu_B$ per atom, the latter being the trivial solution of total spin $S=1/2$. These two solu-

TABLE VII. Same caption as Table VI but for Pd_N clusters.

Cluster	atom	Charge n_{4d}	Charge $N(i)$	Spin m_{4d}	Spin $M(i)$
clusters with equivalent atoms					
Pd_2^{dim}		9.851		0.000	0.000
Pd_3^{tri}		9.788		0.000	0.000
Pd_4^{tetra}		9.410		0.500	0.500
Pd_4^{sq}		9.784		0.000	0.000
Pd_6^{octa}		9.514		0.335	0.333
Pd_{12}^{ico}		9.571		0.169	0.167
Pd_{12}^{cubo}		9.591		0.000	0.000
clusters with inequivalent atoms					
Pd_7^{dipyr}	*a*	9.462	10.018	0.250	0.249
	b	9.560	9.993	0.302	0.301
Pd_8^{mtw}	*a*	9.451	9.997	0.273	0.271
	b	9.675	10.003	0.231	0.229
Pd_9^{bcc}	*a*	9.185	9.991	0.537	0.529
	b	9.592	10.001	0.184	0.184
Pd_{10}^{twp}	*a*	9.538	9.997	0.202	0.200
	b	9.651	10.013	0.204	0.204
Pd_{13}^{ico}	*a*	9.047	9.896	0.619	0.617
	b	9.558	10.009	0.116	0.115
Pd_{13}^{cubo}	*a*	9.035	9.745	0.505	0.503
	b	9.580	10.021	0.125	0.124

tions have nearly the same energy and can be considered as degenerate in view of the accuracy of the method (1–2 meV). These results are consistent with experimental data since for sizes larger than 95 atoms the experimental moment per atom is 0.1 μ_B at most.

The magnetic moment of Pd_{55}^{cubo} is zero or extremely small and undetectable experimentally. For Pd_{55}^{ico} on the contrary, a solution with a magnetic moment of 0.11 μ_B/atom exists but this solution is only 3 meV more stable than the NM one (see Table IX). We therefore did not study larger clusters of palladium since magnetism has almost disappeared for clusters of 55 atoms.

Let us point out that in all sizes we have studied and for both metals the icosahedron is found to be more stable than the cubooctahedron but the energy difference per atom between the two clusters is decreasing when the size increases and thus should reach a crossing point for a larger size.

TABLE VIII. The binding energy per atom E (in eV), the bond length contraction of the equilibrium nearest-neighbor distance relative to the bulk one $\Delta R/R_0$ (in %) and the average magnetic moment M per atom for the ground state and all metastable solutions of large Rh_N clusters.

Cluster	E	$\Delta R/R_0$	M
Rh_{55}^{ico}	4.480	3.7	0.348
Rh_{55}^{cubo}	4.363	1.4	0.345
	4.360	1.4	0.127
Rh_{147}^{ico}	4.814	3.1	0.009
	4.812	3.1	0.216
Rh_{147}^{cubo}	4.751	0.8	0.037

TABLE IX. Same caption as Table VIII but for Pd_N clusters.

Cluster	E	$\Delta R/R_0$	M
Pd_{55}^{ico}	3.150	4.5	0.111
	3.147	4.5	0.000
Pd_{55}^{cubo}	3.093	2.2	0.000
	3.093	2.2	0.032

Even though the tendency to magnetism weakens for large icosahedrons and cubooctahedrons, it is interesting to analyze the distribution of the magnetic moments on the different sites of the cluster. As already pointed out for the thirteen atom clusters, the central atom has a very peculiar behavior. For example, in Rh_{55}^{cubo} and Rh_{55}^{ico} it is the only one bearing a negative moment ($-0.18\ \mu_B$ in Rh_{55}^{ico} and $-0.21\ \mu_B$ in Rh_{55}^{cubo}), whereas in Pd_{55}^{ico} it has a magnetic moment of 0.52 μ_B, i.e., five times larger than the average magnetic moment. In the magnetic solution for Rh_{147}^{ico} the central atom has a moment as large as 0.37 μ_B, whereas its surrounding neighbors have no magnetic moment. These different behaviors of the central atom and its nearest neighbors can be related to their local density of states (LDOS). Indeed, whereas the LDOS on an atom of the first shell rapidly becomes ''bulklike,'' the LDOS on the central atom retains a pronounced discrete character for symmetry reasons. This is illustrated for Rh_{147}^{ico} in Fig. 4(a). Surprisingly, this behavior

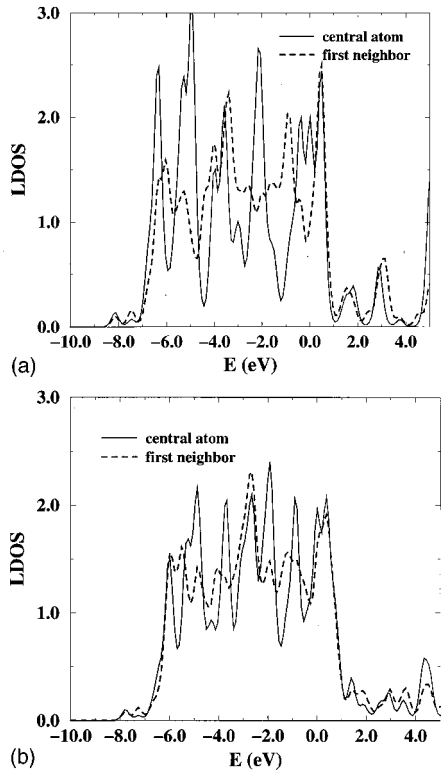

FIG. 4. Local densities of states on the central atom (full line) and on one of its neighbors (dashed line): (a) Rh_{147}^{ico}, (b) fcc Wulff polyhedron Rh_{201}. The discrete levels have been broadened by 0.01 eV.

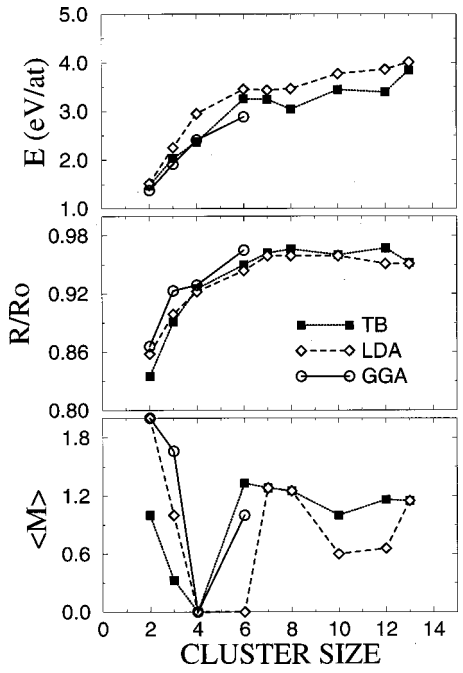

FIG. 5. Comparison of our results (TB, full squares) with LDA (from Ref. 6, diamonds) and GGA (from Ref. 12, empty circles). Upper curves: binding energy per atom, middle curves: equilibrium nearest-neighbor distance R relative to the bulk one R_0, lower curves: average magnetic moment per atom (in μ_B).

is still found for larger centrosymmetric clusters, even when the symmetry is lowered. As an example, we show in Fig. 4(b) the LDOS of the Wulff polyhedron Rh_{201} with an fcc structure. This explains the absence of a local magnetic moment on the first shell while a moment is expected on the central atom when the Fermi level falls in one of the sharp peaks of the LDOS.

As a conclusion, it is difficult to predict the distribution of the magnetic moment in the cluster, since there is a competition between several effects. If the free atom is magnetic like rhodium low coordination should favor higher moments, but the symmetry of a given site and the number of valence *d* electrons are also very important, and of course these effects may play in opposite ways. As can be seen from these few examples the complex experimental magnetic behavior of these clusters is far from being completely elucidated.

C. Comparison with LDA and GGA calculations

The experimental observation of magnetism in Rh_N clusters has stimulated many *ab initio* studies using LDA (Refs. 6–8, 11, and 14) and GGA, (Refs. 12, 13, and 15) whereas for Pd clusters only scarce data can be found in the literature.[6,9–11,14] Therefore, we can present a detailed comparison of our results with those of the *ab initio* methods for Rh only. In Fig. 5, we have plotted the binding energy per atom E, the ratio of the equilibrium nearest-neighbor distance to the bulk one R/R_0, and the magnetic moment per atom M for Rh_N clusters $(0<N<19)$, as obtained in our method and in the LDA (Ref. 7) and GGA (Ref. 13) calculations. Our binding energies are always smaller than those given by LDA, which is known to overestimate this quantity. Actually, our values are on the average closer to the GGA results, except for Rh_6 but a recent GGA calculation by Reddy *et al.*[15] leads to a binding energy (3.28 eV/atom) very close to ours. As already discussed by Barreteau *et al.*,[22] they are more consistent with the values of the surface energies than the LDA ones.

The interatomic distances found in the present work are on the average quite close to the LDA ones, though very slightly larger, but smaller than the GGA results. The latter are presumably overestimated since it is generally admitted[30] that LDA often gives better lattice parameters than GGA.

Finally, the variation of the magnetic moment as a function of size has qualitatively the same shape as in LDA and GGA. Moreover, we must note that for $N=3$, 6, and 12 we have found metastable solutions, close to our ground-state energy, which have the same magnetic moment as in LDA, GGA, and LDA data, respectively. Furthermore, the results for Rh_{19}^{ico} are in good agreement with those of Jinlong *et al.*,[7] since a moment of about 1 μ_B on each atom is found in both cases.

Unfortunately, there is no systematic study of Pd cluster magnetism. In general all existing calculations[6,9–11] show that palladium clusters are either not magnetic, or carry a total moment of 2 μ_B, in agreement with our results. However, a recent calculation by Lee[14] reports a larger magnetic moment (6 μ_B) in Pd_{13}^{cubo} but for a fixed interatomic distance slightly expanded relative to the bulk one that obviously does not correspond to the minimum of total energy.

As a conclusion, the good agreement between our results and those of *ab initio* calculations confirms the validity of our model, the adequacy of its parameters and thus its ability to treat large clusters.

V. SURFACES AND SLABS OF RHODIUM AND PALLADIUM

The possible existence of ferromagnetism in thin films and at surfaces of metals that are nearly ferromagnetic in the bulk (as Rh and Pd for instance) is an interesting issue that has been addressed both theoretically[23–29] and experimentally[31–34] since the decrease of coordination may induce magnetism. This could have important consequences in particular in epitaxial growth, where the element in epitaxy can in addition have its interatomic distance expanded relative to the bulk one. Fink *et al.*[32] seem to find no indication of ferromagnetism in Pd overlayers on Ag(001) in their magnetooptic Kerr-effect measurements but, according to these authors, these experiments may not have a sufficient sensitivity. The low-energy electron diffraction experiments of Quinn *et al.*[48] indicate that the surface layer of Pd(001) relaxes outwards by 3% contrary to all other fcc metals, and they argued that this unusual property could be due to surface ferromagnetism. For rhodium very recent experiments of Goldoni *et al.*[34] found a clear evidence of magnetic ordering at the Rh(001) surface by measuring the linear magnetic dichroism in the angular distribution of Rh-3*d* electrons.

Simple arguments based on the Stoner criterion show that surface effects are playing against magnetism for palladium since the surface LDOS at the Fermi level is smaller than in the bulk, whereas the reverse occurs for rhodium. Magnetic calculations confirm this tendency. Even though, for both elements, surfaces are found non-magnetic within our model

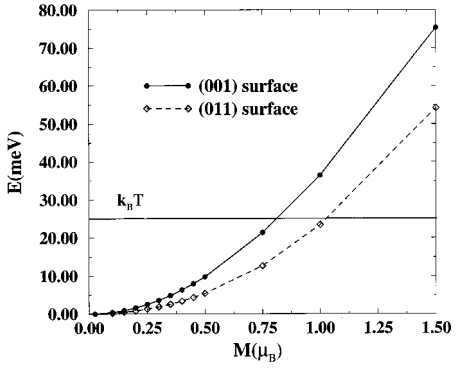

FIG. 6. Total energy per surface atom as a function of magnetic moment per surface atom for 11 layer slabs of Rh with (001) (full line) and (011) (dashed line) orientations. The nonmagnetic state defines the energy zero. The horizontal line indicates the energy $k_B T$ at room temperature.

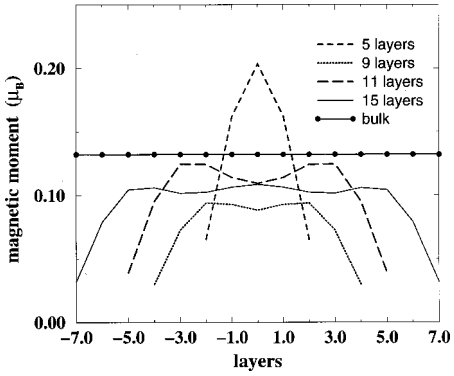

FIG. 7. Magnetic moment (in μ_B/atom) calculated in the tight-binding HF model for (001) Pd slabs of increasing thicknesses and a nearest-neighbor distance of 5.61 a.u. The layer $n=0$ corresponds to the center of the slab. The three-layer and seven-layer slabs are not represented since they are only slightly magnetic. All slab calculations were performed with 36 special $\mathbf{k}_{\|}$ points, and the bulk calculations with 408 special **k** points in their respective irreducible Brillouin zone.

(even under a slight expansion of the first interlayer spacing), when we start our iteration process by introducing a magnetic field the magnetic moment of Pd surface atoms is always much smaller than the bulk one, whereas the opposite behavior is observed for rhodium. This suggests to carry out fixed-spin-moment calculations[29,49] in order to estimate how far in energy the magnetic solution might be for Rh. Figure 6 shows the total energy per surface atom *versus* the magnetic moment per surface atom for (001) and (011) surfaces of 11-layer slabs of Rh, to be compared with Cho and Scheffler[29] results on Rh(001). The agreement is not perfect but quite satisfactory. Indeed their energy shows an almost flat plateau for moments up to $0.6\mu_B$ while, in our calculations, the variation of energy is less than $k_B T$ at room temperature up to moments as large as $0.75\mu_B$ for Rh(001) and $1.0\mu_B$ for Rh(011). Furthermore, the tendency to magnetism of the (011) surface of Rh is even more pronounced than for Rh(001). Thus the (001) and (011) surfaces of Rh are extremely close to magnetism at 0 K. However, note that real surfaces are never perfectly flat but present many defects such as steps, kinks, adatoms, etc. It would be of great interest to determine the influence of these defects that might increase significantly the surface magnetism of Rhodium. Such studies on complex structures are still out of reach of *ab initio* methods but remain very feasible within our model. This will be the subject of a forthcoming publication.

Recently, GGA calculations were carried out on a five-layer ''free-standing'' (001) slab of palladium[30] at the calculated bulk equilibrium distance. An interesting but rather surprising result was obtained: the five-layer slab is magnetic whereas the bulk is not at this distance, but the magnetic moment at the surface is *more than twice smaller* than within the central layer. These two facts seem to be in contradiction. However, we must note that in this work the bulk equilibrium distance is overestimated by 3.6% compared to experiments. For these reasons we decided to perform calculations for various slabs and different expansions in order to get a detailed understanding of the magnetic behavior of this system.

For the five-layer slab, contrary to what was found in Ref. 30, the magnetism appears at an interatomic distance slightly larger than in the bulk. However, the variation of the magnetic moment across the slab is very similar, showing a clear decrease of the magnetic moment at the surface layer (see Fig. 7). We then increased the slab thickness. The interatomic distance was fixed at a given expansion of 8% for which the bulk is clearly magnetic. To our surprise, the convergence to the expanded bulk magnetic moment is far from being monotonic, and magnetism almost disappears for the three-layer and seven-layer slabs. For slabs of nine layers and more the distribution of the magnetic moments starts to stabilize and a bulklike behavior is reached for the fifteen-layer slab (see Fig. 7). However, the magnetic moment at the center of the slab (0.11 μ_B/atom) is smaller than the value we have found earlier in bulk calculations (0.18 μ_B/atom). Actually, the calculations of the bulk was performed with 60 **k** points in the IBZ, and was not fully converged. Increasing the number of special **k** points up to 408 gives a magnetic moment of 0.13 μ_B, much closer to the value found in the slab calculation. It seems that a too small set of **k** points overestimates the magnetic moment. Note that usually *ab initio* calculations are carried out with few layers and at a very small number of **k** points in order to reduce the computer time and thus the convergency on the magnetic moment may not be reached.

Finally, similarly to aggregates, there are two competing effects on palladium surfaces and slabs: atoms with a low coordination present a narrower LDOS, which favors the appearance of a magnetic moment, but their electronic configuration is closer to the d^{10} atomic configuration, which plays against magnetism. Let us recall that the decrease of the number of *d* holes when the average coordination is reduced has already been put forward to explain the evolution of the shape of XVV Auger spectra of small Pd particles as a function of their size.[50]

VI. SUMMARY AND CONCLUSIONS

We have presented a realistic study of the magnetic properties of clusters and slabs of two late $4d$ transition metals, rhodium and palladium, using a tight-binding approach. These metals were chosen as they are known to be NM in the bulk, but exhibit interesting magnetic properties in lower di-

mension. A successful study of these properties was possible by introducing an extension of the tight-binding model, which includes *explicitly* all valence electrons in $4d$ transition metals, i.e., $5s$, $5p$, and $4d$ orbitals. This extension is crucial for the success of the method, as it allows for a charge transfer between the (sp) and d shells and different occupancies of the d orbitals for atoms at inequivalent geometrical positions. Thus it is very difficult to come close to the *ab initio* results with the Hubbard models for pure d states in which the number of d electrons is kept constant.[16–21] Furthermore, even though the magnetic properties are usually correctly predicted when the number of d electrons is well estimated (which may be difficult for instance in Pd), in any case the binding energy per atom is too low, especially for elements at the end of the series, since the contribution of sp electrons is missing. For example in Ref. 17 the bulk energy of Rh is only 3.07 eV instead of 5.78 eV experimentally.

Our results show that magnetic states in the clusters of late $4d$ transition metals occur as a compromise between the binding, the tendency towards atomic behavior at low coordination, and the reduction of electron-electron interaction for polarized d shell relative to free atoms. The driving force for magnetism is the interaction between d electrons, and indeed we found only very small polarization of $5s$ and $5p$ states of magnetic atoms. We have also verified that the same magnetic ground states are stable for the considered clusters even when the Coulomb and exchange interactions between (sp) electrons, or between d and (sp) electrons are neglected. This result is consistent with small average fillings of $5s$ and $5p$ orbitals and confirms that the Coulomb $U_{dd'}$ and exchange $J_{dd'}$ integrals play a dominating role for the magnetic instabilities in transition metals.

We have obtained a very good overall agreement of the calculated properties of Rh_N and Pd_N (up to $N=19$) clusters with the predictions of *ab initio* calculations.[6,12,15] However, the conditions under which a magnetic ground-state sets in are rather subtle, and the Stoner parameter alone, which plays a leading role in the bulk,[40] does not suffice to predict whether a given cluster is magnetic or not, and even more what would be the value of the magnetic moment M. Indeed, many physical effects come into play. It is often argued that, when the coordination is reduced, the LDOS is increased due to band narrowing that tends to induce magnetism according to the Stoner criterion. However, this argument which is roughly valid when the density of states is smooth, may completely fail in a cluster for which the distribution of levels is discrete. Note also that the narrowing of the electronic spectrum is limited by the contraction of bond lengths. As a consequence the details of the electronic structure around the HOMO, in particular the degree of filling of this level and the value of the HOMO lowest unoccupied molecular orbital gap are also very important, and they are determined by many factors: number of atoms, symmetry and bond lengths of the cluster, as well as by the distribution of valence electrons among the s, p, and d orbitals.

The present tight-binding model is very well designed to investigate magnetism in larger clusters, not or only hardly accessible to *ab initio* treatment. Thus, we have been able to study Rh_N clusters up to the size at which they become nonmagnetic. The agreement of our results with experiment is satisfactory since we have found that Rh_N small clusters carry a noticeable magnetic moment up to $N \simeq 100$, which strongly oscillates when size increases.[3,4] However a detailed comparison of these oscillations with those observed experimentally would require the determination of the most stable atomic structure for each size. This determination was not done in this work but could be carried out in the future owing to the simplicity of our method. Palladium has a rather different behavior since the free atom has no magnetic moment. Consequently, there are two competing effects in this metal when the coordination is lowered compared to the bulk one: the narrowing of the LDOS is counteracted by the filling of the d levels when size decreases. This explains the weak tendency to magnetism in Pd_N clusters, as observed experimentally.[3,4]

This method is also very well suited to study magnetism at surfaces and slabs. Our results concerning the (001) surface of Rh are in good agreement with *ab initio* calculations and we predict a reinforced tendency to magnetism for Rh(011). Our studies of palladium slabs show that, on the contrary, the surface is found always less magnetic than the central layer. Unlike the previous implementations of the Hubbard model, which did not include (sp) electrons, it is also realistic enough and might help to understand better certain limitations of the *ab initio* approach.

Let us point out finally that it is feasible to introduce electronic correlations within this model with the help of the perturbation theory[51] or by means of the so called ''local ansatz'' method.[43]

ACKNOWLEDGMENTS

It is our pleasure to thank O. Jepsen, G. A. Sawatzky, and G. Stollhoff for valuable discussions. A.M.O. acknowledges the kind hospitality of DSM/DRECAM/SRSIM, Centre d'Etudes de Saclay, where part of this work was completed, and the support by the Committee of Scientific Research (KBN) of Poland, Project No. 2 P03B 175 14. He also acknowledges the partial support from the Polish-French intergovernment research programme ''Polonium''.

*Electronic address: barreto@atalante.saclay.cea.fr

[1] J. P. Bucher and L. A. Bloomfield, Int. J. Mod. Phys. B **7**, 1079 (1993).

[2] H. Dreyssé and C. Demangeat, Surf. Sci. Rep. **28**, 65 (1997).

[3] A. J. Cox, J. G. Louderback, and L. A. Bloomfield, Phys. Rev. Lett. **71**, 923 (1993).

[4] A. J. Cox, J. G. Louderback, S. E. Apsel, and L. A. Bloomfield, Phys. Rev. B **49**, 12 295 (1994).

[5] K. A. Gingerich and D. L. Cocke, J. Chem. Soc. Chem. Commun. **1**, 536 (1972).

[6] B. V. Reddy, S. N. Khanna, and B. I. Dunlap, Phys. Rev. Lett. **70**, 3323 (1993).

[7] Y. Jinlong, F. Toigo, and W. Kelin, Phys. Rev. B **50**, 7915 (1994).

[8] Y. Jinlong, F. Toigo, W. Kelin, and Z. Manhong, Phys. Rev. B **50**, 7173 (1994).

[9] A. Fahmi and R. A. van Santen, J. Phys. Chem. **100**, 5676 (1996).

[10] M. Harada and H. Dexpert, C. R. Acad. Sci. Paris **322**, 239

(1996).
[11] G. W. Zhang, Y. P. Feng, and C. K. Ong, Phys. Rev. B **54**, 17 208 (1996).
[12] S. K. Nayak, S. E. Weber, P. Jena, K. Wildberger, R. Zeller, P. H. Dederichs, V. S. Stepanyuk, and W. Hergert, Phys. Rev. B **56**, 8849 (1997).
[13] C. H. Chien, E. Blaisten-Barojas, and M. R. Pederson, Phys. Rev. A **58**, 2196 (1998).
[14] K. Lee, Phys. Rev. B **58**, 2391 (1998).
[15] B. V. Reddy, S. K. Nayak, S. N. Khanna, B. K. Rao, and P. Jena, Phys. Rev. B **59**, 5214 (1999).
[16] B. Piveteau, M. C. Desjonquères, A. M. Oleś, and D. Spanjaard, Phys. Rev. B **53**, 9251 (1996).
[17] P. Villaseñor-Gonzales, J. Dorantes-Dávila, H. Dreyssé, and G. M. Pastor, Phys. Rev. B **55**, 15 084 (1997).
[18] J. Dorantes-Dávila, A. Mokrani, H. Dreyssé, and C. Demangeat, J. Magn. Magn. Mater. **165**, 268 (1997).
[19] R. Guirado-López, D. Spanjaard, and M. C. Desjonquères, Phys. Rev. B **57**, 6305 (1998).
[20] R. Guirado-López, D. Spanjaard, M. C. Desjonquères, and A. M. Oleś, Eur. Phys. J. B **3**, 437 (1998).
[21] R. Guirado-López, D. Spanjaard, M. C. Desjonquères, and F. Aguilera-Granja, J. Magn. Magn. Mater. **186**, 214 (1998).
[22] C. Barreteau, D. Spanjaard, and M. C. Desjonquères, Phys. Rev. B **58**, 9721 (1998).
[23] C. L. Fu, A. J. Freeman, and T. Oguchi, Phys. Rev. Lett. **54**, 2700 (1985).
[24] S. Blügel, M. Weinert, and P. H. Dederichs, Phys. Rev. Lett. **60**, 1077 (1988).
[25] M. J. Zhu, D. M. Bylander, and L. Kleinman, Phys. Rev. B **43**, 2874 (1990).
[26] M. J. Zhu, D. M. Bylander, and L. Kleinman, Phys. Rev. B **45**, 4007 (1991).
[27] O. Eriksson, R. C. Albers, and A. M. Boring, Phys. Rev. Lett. **66**, 1350 (1991).
[28] I. G. Batirev, J. A. Leiro, and T. Oguchi, Philos. Mag. Lett. **73**, 385 (1996).
[29] J.-H. Cho and M. Scheffler, Phys. Rev. Lett. **78**, 1299 (1997).
[30] F. Delbecq and P. Sautet, Phys. Rev. B **59**, 5142 (1999).
[31] C. Rau, G. Xing, and M. Robert, J. Vac. Sci. Technol. A **6**, 579 (1988).
[32] R. L. Fink, A. Ballentine, J. L. Erskine, and J. A. Araya-Pochet, Phys. Rev. B **41**, 10 175 (1990).
[33] S. C. Wu, K. Garrison, A. M. Begley, F. Jona, and P. D. Johnson, Phys. Rev. B **49**, 14 081 (1994).
[34] A. Goldoni, A. Baraldi, G. Comelli, S. Lizzit, and G. Paolucci, Phys. Rev. Lett. **82**, 3156 (1999).
[35] J. C. Slater and G. F. Koster, Phys. Rev. **94**, 1498 (1954).
[36] M. J. Mehl and D. A. Papaconstantopoulos, Phys. Rev. B **54**, 4519 (1996).
[37] A. R. Williams, J. Kübler, and C. D. Gelatt, Jr., Phys. Rev. B **19**, 6094 (1979); P. M. Openeer, T. Maurer, J. Sticht, and J. Kübler, *ibid.* **45**, 10 924 (1992).
[38] V. I. Anisimov, J. Zaanen, and O. K. Andersen, Phys. Rev. B **44**, 943 (1991); V. I. Anisimov, M. A. Korotin, J. Zaanen, and O. K. Andersen, Phys. Rev. Lett. **68**, 345 (1992).
[39] C. Barreteau, D. Spanjaard, and M. C. Desjonquères, Surf. Sci. **433-435**, 751 (1999).
[40] A. M. Oleś and G. Stollhoff, Phys. Rev. B **29**, 314 (1984); G. Stollhoff, A. M. Oleś, and V. Heine, *ibid.* **41**, 7028 (1990); Phys. Rev. Lett. **76**, 855 (1996).
[41] D. van der Marel and G. A. Sawatzky, Phys. Rev. B **37**, 10 674 (1988).
[42] U. von Barth and L. Hedin, J. Phys. C **5**, 1629 (1972).
[43] A. M. Oleś, Phys. Rev. B **28**, 327 (1983).
[44] V. L. Moruzzi, J. F. Janak, and A. R. Williams, *Calculated Properties of Metals* (Pergamon Press, New York, 1978).
[45] V. L. Moruzzi, P. M. Marcus, and P. C. Pattnaik, Phys. Rev. B **37**, 8003 (1988).
[46] V. L. Moruzzi and P. M. Marcus, Phys. Rev. B **39**, 471 (1989).
[47] M. C. Desjonquères and D. Spanjaard, *Concepts in Surface Physics* (Springer-Verlag, Berlin, 1996), and references therein.
[48] J. Quinn, Y. S. Li, D. Tian, H. Li, F. Jona, and P. M. Marcus, Phys. Rev. B **42**, 11 348 (1990).
[49] K. Schwarz and P. Mohn, J. Phys. F **14**, L129 (1984).
[50] B. Bellamy, A. Masson, V. Degouveia, M. C. Desjonquères, D. Spanjaard, and G. Tréglia, J. Phys.: Condens. Matter **1**, 5875 (1989).
[51] G. Tréglia, F. Ducastelle, and D. Spanjaard, J. Phys. (France) **41**, 281 (1980); **43**, 341 (1982).